Biomolecular modifications during keratinocyte differentiation: Raman spectroscopy and chromatographic techniques

Joudi Bakar, Rime Michael-Jubeli, Sana Tfaili, Ali Assi, Arlette Baillet-Guffroy, Ali Tfayli

Analyst

Accepted Manuscript

This article can be cited before page numbers have been issued, to do this please use: J. bakar, R. Michael-Jubeli, S. Tfaili, A. ASSI, A. Baillet-Guffroy and A. Tfayli, *Analyst*, 2021, DOI: 10.1039/D1AN00231G.

View Article Online
DOI: 10.1039/D1AN00231G

Biomolecular modifications during the keratinocytes differentiation: Raman spectroscopy and chromatographic techniques.

Joudi Bakar, Rime Michael-Jubeli*, Sana Tfaili*, Ali Assi, Arlette Baillet-Guffroy, Ali Tfayli

Lipides : systèmes analytiques et biologiques, Université Paris-Saclay, 92296 Châtenay-Malabry, France.

Author(s):

1- Joudi Bakar : joudi.bakar@u-psud.fr, Université Paris-Saclay, Lipides : systèmes analytiques et biologiques, 92296, Châtenay-Malabry, France.

2- Rime Michael-Jubeli : **This author accepts correspondance and proofs**, rime.michael-jubeli@u-psud.fr, Université Paris-Saclay, Lipides : systèmes analytiques et biologiques, 92296, Châtenay-Malabry, France. Orcid ID : 0000-0002-2944-5295.

3- Sana Tfaili : **This author accepts correspondance and proofs**, sana.tfaili@u-psud.fr, Université Paris-Saclay, Lipides : systèmes analytiques et biologiques, 92296, Châtenay-Malabry, France. Orcid ID : 0000-0002-6256-6777

4- Ali Assi: ali.assi@u-psud.fr Université Paris-Saclay, Lipides : systèmes analytiques et biologiques, 92296, Châtenay-Malabry, France.

5- Arlette Baillet-Guffroy: arlette.baillet-guffroy@u-psud.fr, Université Paris-Saclay, Lipides : systèmes analytiques et biologiques, 92296, Châtenay-Malabry, France.

6- Ali Tfayli : ali.tfayli@u-psud.fr, Université Paris-Saclay, Lipides : systèmes analytiques et biologiques, 92296, Châtenay-Malabry, France.

***Corresponding authors**: Sana Tfaili, 5 rue Jean-Baptiste Clément - 92290 Châtenay-Malabry – France, Tel: +33146835463, fax: +33 Fax: +33149835458, sana.tfaili@u-psud.fr

Rime Michael-Jubeli, 5 rue Jean-Baptiste Clément - 92290 Châtenay-Malabry – France, , Tel: +33146835904, fax: +33 Fax: +33149835458, rime.michael-jubeli@u-psud.fr

View Article Online
DOI: 10.1039/D1AN00231G

Abstract

From basal layer until *stratum corneum*, lipid and protein biomarkers associated to morphological changes denote keratinocytes differentiation and characterize each epidermis layer. Herein, we followed keratinocytes differentiation in early stages on HaCaT cells over a period of two weeks by two complementary analytical techniques: Raman microspectroscopy and High-Performance Liquid Chromatography coupled to High resolution Mass Spectrometry. High concentration of calcium in the medium induced HaCaT differentiation *in vitro.* Results from both techniques underlined keratinocytes passage from granular layer (Day 9) to *stratum corneum* layer (Day 13). After 13 days of differentiation, we observed a strong increase in lipids content, decrease in proteins, decrease in DNA, and a decrease in glucosylceramides/ceramide and sphingomyelins /ceramides ratios.

Keywords: Keratinocytes differentiation, Raman microspectroscopy, HPLC/HR-MS, lipid biomarkers.

View Article Online
DOI: 10.1039/D1AN00231G

Abbreviation

APPI: Atmospheric Pressure PhotoIonization

CER: Ceramide

D: Differentiation Day

FFA: Free Fatty Acids

HPLC: High-Performance Liquid Chromatography

HR-MS: High-Resolution Mass Spectrometry

NPLC: Normal-Phase Liquid Chromatography

SC: *Stratum Corneum*

SG: *Stratum Granulosum*

View Article Online
DOI: 10.1039/D1AN00231G

Introduction:

Epidermis – the outermost layer of the skin – consists of several stratified layers of keratinocytes: basal, spinous, granular and cornified layers[1]. These layers differ by their thickness, their cells morphology, the proliferative activity and the expression of different differentiation markers[2]. The basal layer (*stratum basale*) consists of large and columnar cells – epidermal stem cells –attached to the basement membrane by hemidesmosomes[3]. Stem cells have a proliferative activity and give rise to cells that can migrate and differentiate through the three other layers[4]. The spinous layer (*stratum spinosum*) is a suprabasal layer. Cells of this layer are attached together by desmosomes[5]. In the granular layer (*stratum granulosum*), keratohyalin granules and lamellar bodies appear, the latter are rich in lipids and catabolic enzymes. Lamellar bodies fuse with plasma membrane and release their lipid content at the interface between the granular and cornified layers. The secreted lipids are rearranged and assembled into lamellar structure. These structures fill the intercellular region of *stratum corneum* (SC) and surround the corneocytes to form a compact intercorneocytes matrix which plays a key role in skin barrier function[3, 6]. When the keratinocytes reach the uppermost layer of the skin (SC), they lose their capacity for cell division, lose their nucleus and acquire a flatter shape to become corneocytes. Corneocytes are packed with keratin filaments and embedded in a lipid matrix organized in lamellae consisting mainly of long-chain ceramides (CER), free fatty acids (FFA), and cholesterol[6, 7] .

Keratinocytes differentiation stages go together with morphological changes. These changes are generally confirmed biochemically by immunoblotting and immunofluorescence of proteins and genes known as differentiation markers in the epidermis such as keratin 1 involucrin, and filaggrin[8]. In parallel with protein modifications and morphological changes, lipids composition and concentrations evolve along differentiation. In fact, epidermal lipid biosynthesis is initiated at early stage of keratinocytes differentiation. Ceramides are generated in the endoplasmic reticulum of *Stratum Granulosum* (SG) cells, they consist of fatty acid chains linked to sphingoid bases via amide bonds[9-11] .

View Article Online
DOI: 10.1039/D1AN00231G

Ceramide biosynthesis increases along keratinocytes differentiation, ceramides are subjected to changes – probably to avoid their intracellular cytotoxicity level – in the Golgi apparatus; *i.e./* glycosylation to give the glucosylceramides and phosphorylation to generate Sphingomyelins[11]. The glucosylceramides and Sphingomyelins are then packaged into epidermal lamellar bodies (LB).

At the interface between the SG and SC, lamellar bodies release their lipid content of glucosylceramides and sphingomyelins. b-glucocerebrosidase and sphingomyelinase convert back respectively glucosylceramides and sphingomyelins to their ceramides species[3, 6]. Therefore, ceramides are identified as SC markers, and glucosylceramides and sphingomyelins are identified as SG markers in keratinocytes differentiation stages.

Spontaneously immortalized Human cell line HaCaT – often used as a keratinocytes model – are near to normal phenotype, possess the capacity of proliferating and differentiating, and exhibit all major differentiation surface markers[8, 12]. Primary human keratinocytes are perfect to study differentiation; but some drawbacks such as slow growth rate complicate cell culture and prevent long-term investigation of differentiation signals[12-14]. HaCaT cells have the advantage to permit following differentiation process during a long period (two weeks).

Several modifications of culture medium conditions are described to stimulate keratinocytes differentiation *in vitro* [15]. Ionic calcium has been shown to be a major agent in controlling keratinocytes differentiation *in vitro* and *in vivo*, it stimulates lamellar bodies migration which secret their lipid content at interface between the SG and SC[6, 16].

In this work, HaCaT cells were first cultured in a low calcium medium to induce dedifferentiation then they were subjected to a high calcium concentration (2.8 mM) medium to induce their differentiation during a period of 13 days *in vitro*. The differentiation process was followed using Raman spectroscopy which enables a direct molecular characterization with no labeling[17]. Raman spectroscopy enables following cells differentiation at single cell level. In addition to the advantage of Raman as a free label diagnostic technique,

View Article Online
DOI: 10.1039/D1AN00231G

it provides a phenotype-specific biomolecular fingerprint for the different molecular components in the sample. Complementary information was obtained using High-performance Liquid Chromatography coupled to High Resolution Mass Spectrometry (HPLC/HR-MS) and (HPLC/Corona) permitted to follow lipid biomarkers evolution classes (ceramide, glucosylceramides and sphingomyelins). These two analytical methods are complementary and constitute an efficient methodology to study differentiation biomolecular changes and to determine keratinocytes differentiation stages.

Materials and methods

1- Cell culture

HaCaT cells were cultured in DMEM High Glucose, calcium and serum free media (Life Technologies), and supplemented with 10% fetal bovine serum (sigma) treated with Chelex 100 to remove endogenous calcium, 100 U⁄mL of penicillin, 100 µg⁄mL of streptomycin, 2% glutamine solution 200mM (Sigma) and 1% of calcium chloride solution 3mM (Sigma) to obtain a final concentration of 0.03mM. HaCaT cells were maintained for at least 3 weeks in low calcium media to dedifferentiate to the basal phenotype [18]. High calcium concentration induces a rapid morphological change of keratinocytes *in vitro*[1, 12]. To induce the differentiation, the low-calcium medium (0.03mM) was replaced by a high-calcium medium (2.8 mM as final concentration). Cultures were maintained at 37C° in a humidified atmosphere with 5% CO_2. Since the HaCaT cells are very sensitive to cell density, cells in low calcium medium should be detached using trypsin-EDTA when they reach 70% confluence, otherwise they may start to differentiate at higher density[8]. The HaCaT cells were graciously obtained from Nanomédicaments et nanosondes laboratory, Tours University; France (Source: Thermo Fisher scientific, Les Ulis, France).

1.1- Cell culture preparation for Raman microspectroscopy analyses

The differentiation process of HaCaT keratinocytes was followed over 13 days. For Raman analysis, CaF_2 windows were introduced in well plates during cell culture. To reach the required cell density at each differentiation day, basal HaCaT cells were seeded in a 24 well plate on sterile CaF_2 windows. Cells were

View Article Online
DOI: 10.1039/D1AN00231G

deposited in a descending order: reducing number of cells compensates continuing cell proliferation occurring during differentiation process and permits to harvest cells subsequently.

HaCaT were first cultured for 24 h under a low calcium medium to allow cells adhesion. After 24 h, the low-calcium medium was replaced with high-calcium medium to initiate the differentiation process. The medium was changed every three days. At each collection step 2 hours, 3, 6, 9 and 13 days, HaCaT cells were washed twice with phosphate buffered saline (PBS) and then fixed with formalin (4%, 15 min). Cells fixed on CaF2 window were then washed again with PBS and water.

1.2- Cell culture preparation for HPLLC/HR-MS, HPLC/corona analyses

A decreased density of cells was seeded directly – without CaF_2 windows – into 75-cm^2 flasks in presence of low calcium medium and incubated for 24h in 5% CO_2, 37C°. Decreased cells density permits to not exceed 60-70% of confluence at each collection step. To follow the changes in lipid composition during keratinocytes differentiation process, the low calcium medium was replaced after 24h by the high one and maintained for 13 days.

2- Raman microspectroscopy

2.1- Instrumentation Raman spectrometer

Raman spectral acquisition and spectral imaging were collected using a Labram HR microspectrometer (Horiba scientific, Palaiseau, France). A 633 nm He:Ne laser (Toptica Photonics, Munich, Germany) giving a 10 mW power on the sample was used. The laser beam was focused using a 100X short focal microscope objective (Olympus, Tokyo, Japan). The collected light was filtered with a Edge filter and dispersed with a 4 cm^{-1} spectral resolution using a 300 µm slit and 300 grooves/mm holographic grating. The Raman Stokes signal was recorded with a Synapse Charge-Coupled Device detector: CCD camera (Andor Technology, Belfast, UK) containing 1024x256 pixels. Spectral acquisition was performed using Labspec 6 software (Horiba Scientific, Lille, France). Raman measurements were performed on the SC surface in the 400–3800 cm^{-1} spectral range. For each spectrum the acquisition time was 2 x 5 seconds. The used experimental set-up enables to reach spatial resolution down to 0.5x0.5 μm^2. The resolution limit depends on the Rayleigh

View Article Online
DOI: 10.1039/D1AN00231G

diffraction criterion and can be defined by the laser wavelength and the numerical aperture of the microscope objective. The other determining factor for the spatial resolution is the chosen step size for mapping. In this study, we have used a 1x1µm² (for X and Y lateral steps).

2.2- Raman spectral processing

Acquisition and pre-processing of all spectra were performed using a Labspec 6 software (Horiba Scientific, Palaiseau, France). All spectra were subjected to the same pre-processing protocol. All spectra were smoothed using Savitzky-Golay algorithm (4th order, 9 points), normalized by applying unit vector method and baseline corrected using an automatic polynomial function. To follow the significant variations in cells spectra, Kruskal-wallis (a non-parametric test) was applied using in house developed software with Matlab (Mathworks, Natick, MA, USA).

For spectral imaging, single cells were scanned with 1 µm step (X and Y) with an acquisition time of 2x5 seconds for each point.

3- Lipid extraction

Cells were dispersed using trypsin-EDTA, then cell pellets were dissolved in 600 µL of distilled water, mixed with a magnetic stirrer for 10 minutes at room temperature. Total lipids were extracted by the modified method of Bligh and Dyer [19]. Briefly, 1.5 mL of methanol was added and vortexed for 2 minutes. Then, 3 mL of chloroform containing 1-Eicosanol as an internal standard (0.3 mg/mL on chloroform) was also added, the mixture was incubated for 1 hour at room temperature in the dark. The organic phase was collected and evaporated under a stream of nitrogen, then lipid residues were resuspended with 100 µL of chloroform[20, 21] .

View Article Online
DOI: 10.1039/D1AN00231G

4- Instrumentation and analytical method (HPLC/corona and HPLC/HR-MS) for biomarkers analysis

The analysis of the extracted lipid was conducted by HPLC (Dionex Ultimate 3000, ThermoFisher Scientific, San Jose, CA). Separation of lipid occurred in NPLC using (PVA)-Sil column (PVA-bonded column; 5 µm particle size, 150 × 4.6 mm) purchased from YMC (Kyoto, Japan). A solvent gradient of Heptane/ethyl acetate (99.8: 0.2 v/v) (Solvent A), acetone and ethyl acetate (2: 1 v/v) with acetic acid (0.02% v/v) (Solvent B) and 2-propanol/ water (85:15v/v) (with acetic acid and ethanolamine each at 0.025% v/v) (solvent C) were used. Flow rate was set to 1 mL/min and injected volume was 10 µL. Detection was performed using two detectors simultaneously: a Corona CAD® and a hybrid mass spectrometer LTQ-Orbitrap Velos Pro (Thermo Fisher Scientific, San Jose, CA) equipped with an Atmospheric Pressure Photoionization (APPI) source. APPI positive ion mode was used to analyze the extracted lipid. The mass scan range was 220-1800 atomic mass units (amu). A full scan detection mode and fragmentation was performed by the orbital trap at a resolution of 100 000. The analytical conditions are detailed in a previous work[21] .

Results:

1- Morphological evolution

The first step of the study consisted of the dedifferentiation of the HaCaT cells by incubating them in a low calcium concentration medium (0.03) mM for 3 weeks. Non differentiated keratinocytes (ND) had a morphology closer to the spindle shape. They are less compacted and with no contact between cells as shown in figure 1(A). In order to induce HaCaT cells differentiation process, medium was replaced by a high calcium concentration medium (2.8 mM). As shown in figure 1 (B), morphological changes were observed following the keratinocytes differentiation. After 2H of exposure, cells began to exhibit a more cuboidal shape with close packing. Fusiform cells were detected at D9 and D13 days (orange arrows in figure 1 (B)). Stratified layers appeared from D9 and became thicker at D13. Cells overlapped at D13 and made impossible to determine the limit at individual cell level (Day 13 in figure 1 (B) and figure 3).

View Article Online
DOI: 10.1039/D1AN00231G

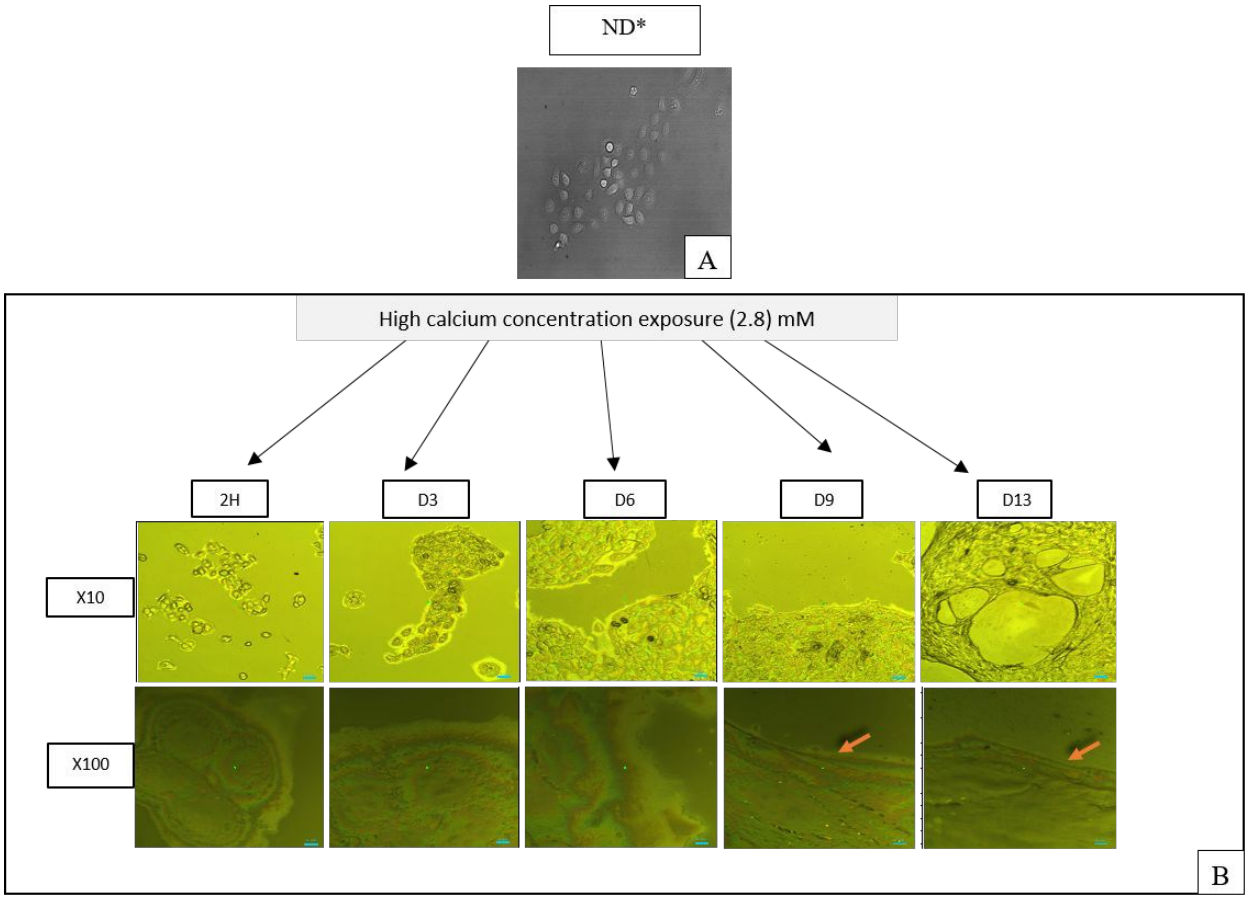

Figure 1: Morphological evolution of HaCaT cells during the differentiation process. A) Microscopic image after 3 weeks of incubation in low calcium concentration medium (0.03 mM). B) White light images (x10, and x100) during different period (2H, 3, 6, 9, and 13 days) of incubation in high calcium concentration medium (2.8 mM). Morphological modification in the cellular shape was observed. The orange arrows point the formation of fusiform cells and the stratified layers which appeared at D9 and became thicker at D13. ND: undifferentiated HaCaT, h: hours, D: days.*

1- Raman spectroscopy: Spectral features of HaCaT cells

The spectral signatures of HaCaT cells at each differentiation day were achieved using Raman microspectroscopy. In order to focus on the evolution of lipids along differentiation, spectra from cytoplasm were collected. Figure 2 illustrates mean cytoplasm spectra at each differentiation day. The presence of a band at 960 (953-978) cm $^{-1}$ can visually be observed on the spectra. The 960 cm^{-1} band appeared after 6 days of differentiation and clearly increased after 13 days. Spectra collected at D13 on stratified layers showed the highest integrated intensities of this band compared to other regions. The 960 cm^{-1} band could be assigned to an increase in saturated ceramides amounts, as it was mentioned in a comparative study

View Article Online
DOI: 10.1039/D1AN00231G

between unsaturated and saturated ceramides[22]. Another possible assignment could be an increase in the keratin level based on the band attribution in[23] table 1.

In order to highlight significant spectral modifications, Kruskal-Wallis was applied between spectra issued from cells at different differentiation days. P-value was fixed to 0.05 and the spectral regions showing significant variations were identified and listed in table 1.

A decrease in the bands related to phospholipids at D3 (598 cm^{-1}, 831 cm^{-1} (ν_{asym} O-P-O)), followed by a slight increase at D6. While no changes in phospholipids were observed between D6 and D9, a marked decrease was shown at D13 (598 cm^{-1}, 831 cm^{-1} (ν_{asym} O-P-O)) (table 1). The decrease in the phospholipids relative content between D0 and D3 can also be observed by following alkyl chain related vibrations: νCC (1086 cm^{-1}), δ CH_2 twisting (1305 cm^{-1}) and δ CH scissoring (1448 cm^{-1}).

The observation of cholesterol and cholesterol esters related bands showed no modification at D3 while higher intensity appeared at D6 (700 cm^{-1}) and the increase continued for D9 (607 cm^{-1}). Cholesterol and cholesterol esters are known to markedly increase in the SG.

The most marked evolution was observed in the spectral features related to lipid chains between D9 and D13 by mainly a high marked increase in the CH_2 stretching bands (2851 and 2882 cm^{-1}). This increase was also observed for CC stretching (1086 cm^{-1}) and δ CH_2 twisting (1305 cm^{-1}). Lipid increase may be related to an advanced stage in the differentiation *i.e.* the transition between SG and SC. The decrease in the δ CH scissoring (1448 cm^{-1}) was more related to conformational modifications in other molecular components (proteins) than lipids[24].

The 3059 cm^{-1} band (=CH stretching) showed a continuous decrease in unsaturated moieties from D6 till D13.

In addition to the modifications observed in the lipid related spectral features, changes were observed for other molecular features. For instance, between D9 and D13, a marked decrease was automatically identified

View Article Online
DOI: 10.1039/D1AN00231G

by Kruskal-Wallis in the spectral region (705-736 cm^{-1}) assigned to nucleic acids (table 1). DNA variation accords with the observations obtained from lipid related bands suggesting the end of SG phase (figure 3).

An interesting observation was also shown for amino-acids and protein related features. From D0 to D3, significant decreases were observed for amino-acids related bands, *i.e.* cytosine (νCS at 669 cm^{-1}), tryptophan (ring breathing at 760 cm^{-1}), tyrosine (855 cm^{-1} (ring breathing), 1044 cm^{-1}) and proline (855 cm^{-1}). The decrease in the proteins spectral signature contributes in the decrease in the CH scissoring band at 1448 cm^{-1}.

From D3 to D6, the significant changes in proteins are mostly structure related. For instance, the increase in the 960 cm^{-1} band was explained by an increase in the β-sheets in keratin (table 1). In parallel, a shift to higher wavenumbers of the symmetric CH_3 stretching band can be associated with unfolding of proteins. The modifications in the secondary structure of proteins was also observed from D6 to D9 with an increase in the α helix related sub-band in the Amide I band (table1). An increase in the CH scissoring occurred also.

Finally, at D13, a decrease in the relative intensities of CH_3 stretching bands mainly associated to proteins is observed. This was described previously[25, 26] and is associated to skin barrier function.

View Article Online
DOI: 10.1039/D1AN00231G

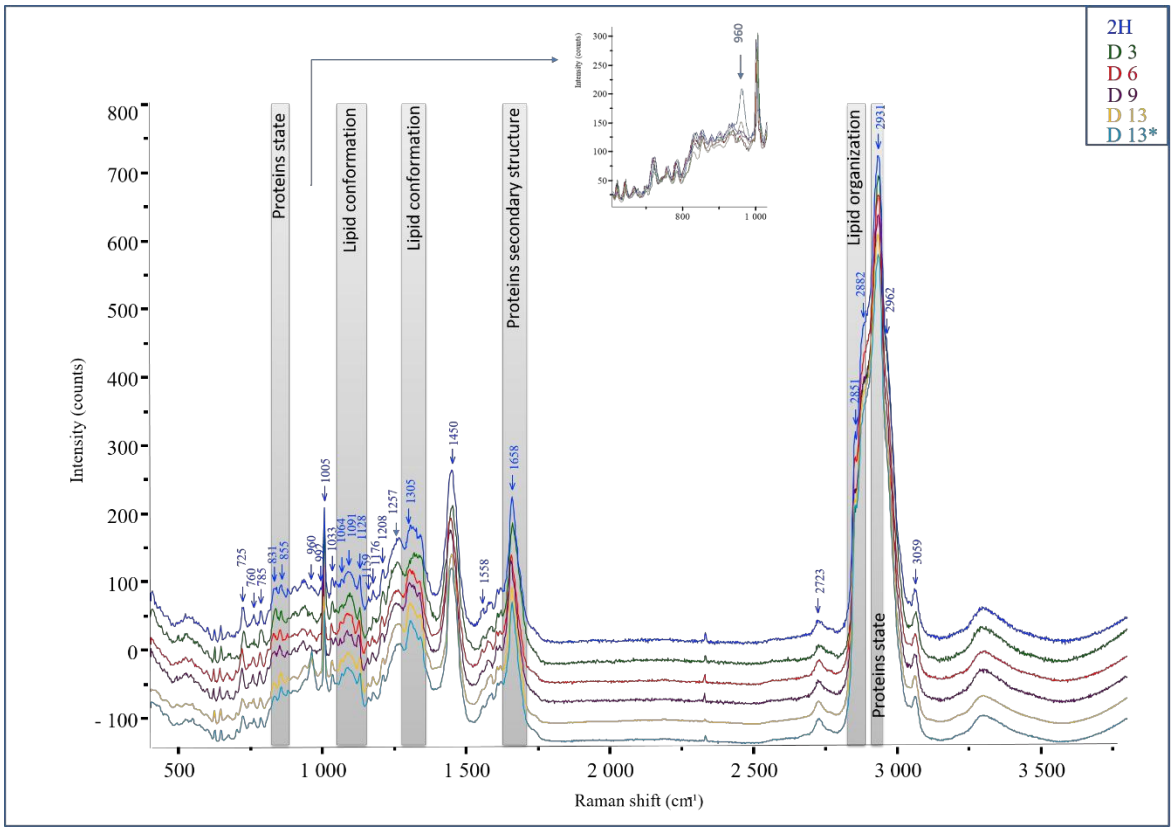

Figure 2: At each differentiation day, the mean cytoplasmic spectrum of several cells was calculated (n=12). The mean spectra of HaCaT obtained after high calcium concentration exposure at (2H, 3, 6, 9, and 13 days) were compared. Several modifications were observed between the differentiation days. A clear increase in the peak intensity at 960 cm^{-1} was detected at D13 (yellow spectrum) and particularly on the stratification layers (light blue spectrum). mean spectrum of HaCaT at D13, taken from the stratified layers.*

Table 1 : Assignment of spectral bands in a Raman spectrum of HaCaT cells during the differentiation process. ν elongation or stretching, δ deformation.

Wavenumber (cm^{-1})	2H vs D3	D3 vs D6	D6 vs D9	D9 vs D13	Assignment
598 (592-605)	↘	↗	-	↘	Phospholipids[27]
607 (605-614)	-	-	↗	-	Cholesterol[28]/Glycerol[29]
669 (661-676)	↘	-	-	-	ν (C-S) of cytosine[30]
700 (693-705)	-	↗	-	-	Cholesterol, cholesterol ester[23]
725 (705-736)	-	-	-	↘	Ring breathing mode of DNA /RNA bases[27, 30]
760 (746-768)	↘	↗	-	-	Ring breathing tryptophan[30, 31]
831 (823- 844)	↘	-	-	↘	ν_{asym} (O-P-O) [30]/Out-of-plane ring breathing, tyrosine[31]
855 (846-871)	↘	-	-	-	Ring breathing mode of tyrosine & ν(C–C) of proline ring[31]
960 (953-978)	-	↗	-	↗↗	**ν** (C–C) β-sheet keratin conformation[23]. ν C–N[22]
1044 (1040-1053)	↘	-	-	-	Tyrosine[32]
1086 (1073-1100)	-	-	-	↗	νC–C, lipid chains[30, 31]
1128 (1116-1140)	↘	-	-	-	νC–C, lipid chains[28, 33]
1305 (1284-1320)	↘	-	-	↗	δCH_2 twisting (lipid)[30, 34]
1448 (1406-1494)	↘	-	↗	↘	δC-H scissoring (proteins and lipid)[30, 34]
1558 (1538-1564)	-	-	-	↗	Tryptophan[35]

View Article Online
DOI: 10.1039/D1AN00231G

1658 (1630-1744)	-	-	↗↗	-	ν (C=O) amide I, α helix of keratin[23]. Little contribution for ν(C=C) lipid[34, 36]
2723 (2697-2755)	-	-	-	↘	ν (CH) aliphatic[33]
2851 (2833-2856)	-	-	-	↗↗	Lipid, ν_{sym} (CH_2)[36-38]
2882 (2856-2895)	-	-	-	↗↗	Lipid, ν_{asym} (CH_2)[27, 37]
2931 (2902-2953)	-	2934	-	↘	ν_{sym} (CH_3)[33]
2962 (2953-3000)	-	-	-	↘↘	ν_{asym} (CH_3)[30, 33]
3059 (3047-3080)	-	↘	↘	↘	ν(=CH) of lipid[36, 39]

2- Raman microspectroscopy: Spectral images of HaCaT cells

In parallel with spectral analyses, spectral imaging was performed in order to monitor possible sub-cellular changes along with the differentiation days and false-colored images were obtained (figure 3).

In the first column of figure 3, the evolution of DNA to lipid content can be monitored by following the (773-790 cm^{-1}) / (2820-2890 cm^{-1}) ratio.

At D0, after 2 hours of exposure to high calcium concentration medium, nucleus can be clearly identified in green (light blue). Based on the color bar, the pixels presented in green (light blue) are indicative to higher ratio values than dark blue ones. A decrease in the ratio values was observed starting at D6 where the nucleus remained clearly identified. At D9, the decrease of DNA is clearly observed, and the identification of nucleus is much difficult. Finally, at D13, nucleic acids disappeared (figure 3, first column).

The second column of figure 3 illustrates the lipid to protein ratio (2820-2890 cm^{-1})/ (2900-2970 cm^{-1}). After 2H of high calcium exposure, lipid / protein ratio seems to record the highest intensity (red color) at the cell membrane area, indicating the localization of the lipid at a high level at the cell membrane zone. After 3 days of differentiation, the red color begins to disperse throughout the cell except the nucleus zone. In addition, at this differentiation day a very high intensity zone was detected which may reflect the localization of a very high amount of lipid content. Egawa *et al.,* also observed strong signal intensities of lipid surrounding the nucleus (2850 cm^{-1}) and related it to endoplasmic reticulum synthesis of lipid[40]. At D6 and D9, we can clearly see a decrease in the intensity of this ratio in the cytoplasm. In contrast, higher values started to be observed in the nucleus at D6 and continued to increase at D9. At D13, the lipid/protein distribution is more homogenous all over the images with high values. This is in concordance with results

View Article Online
DOI: 10.1039/D1AN00231G

obtained from spectral analyses (table 1) and with Egawa *et al.* observation at the final stage of Keratinocytes differentiation. At this stage, Keratinocytes with digested nuclei form layered structures and present a flattened shape with strong signal intensity of lipids (2850 cm^{-1})[40].

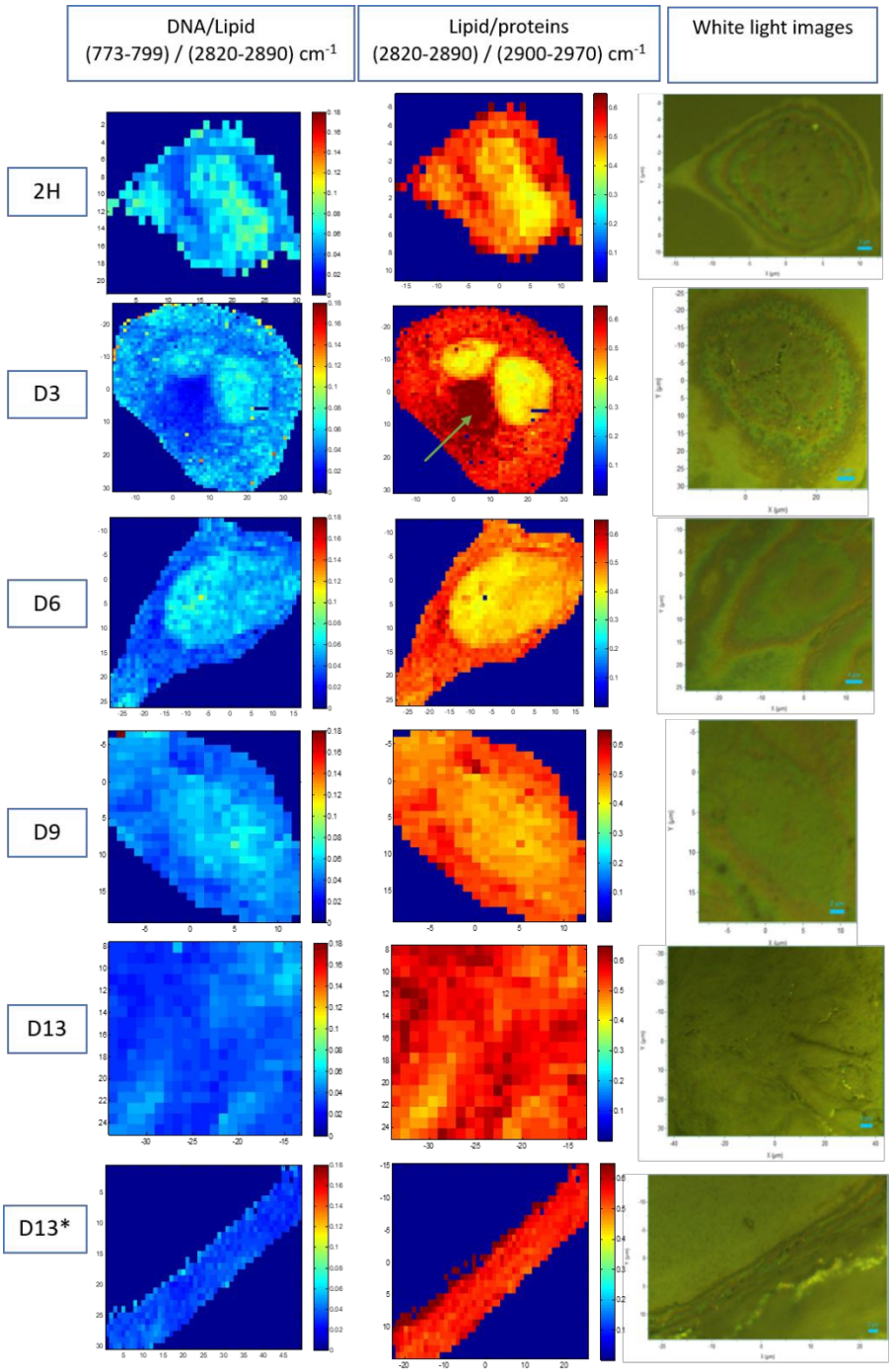

*Figure 3: False-colored Raman images of HaCaT during different period after high calcium exposure. The evolution of DNA/lipid ratio (733-799/2820-2890) cm^{-1} and lipid /protein ratio (2820-2890/2900-2970) cm^{-1} was followed during the differentiation. The green arrow indicates the localization of a high lipid content. *Stratified layers.*

View Article Online
DOI: 10.1039/D1AN00231G

3- Lipid biomarkers evolution by HPLC/Corona & HPLC/HR-MS

Ceramides, glucosylceramides and sphingomyelins classes are considered as lipid biomarkers of differentiation stages. The analytical method used in this study was previously developed by our group [21] and enables to separate epidermis lipid classes in one single run (data not shown). Using this method, we have followed epidermal lipid biomarkers evolution during keratinocytes differentiation. As shown in figure 4, the ratios of chromatographic peak area of glucosylceramides/ceramides and sphingomyelins/ceramides increased throughout the differentiation until reaching a maximal value at D9. A marked decrease of these ratios can be observed at D13.

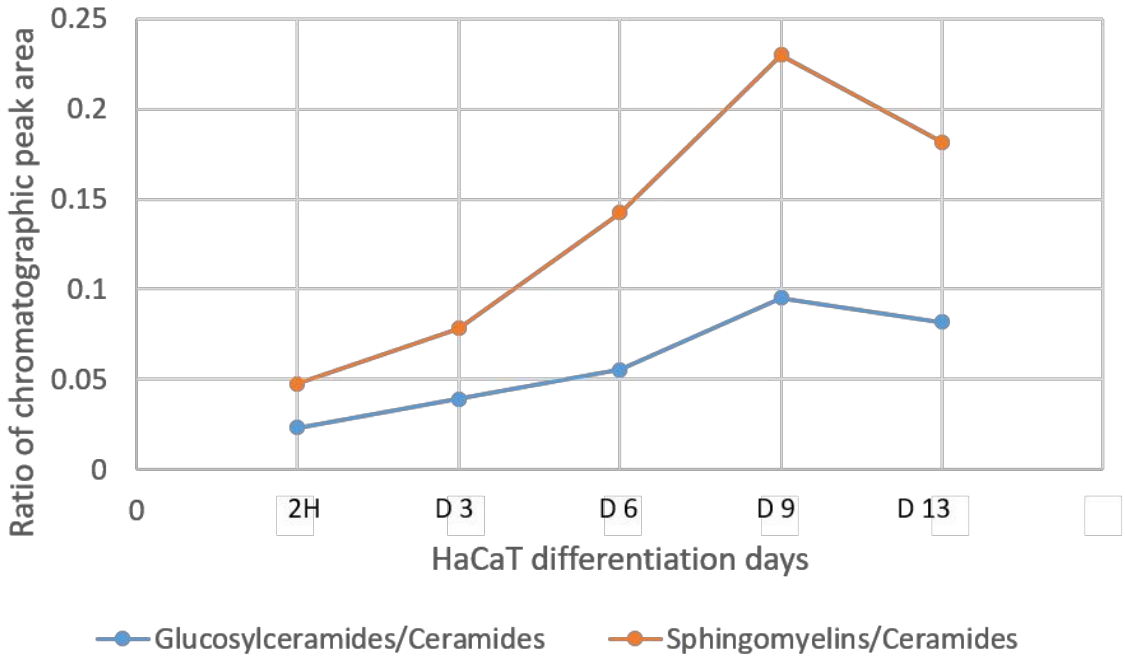

Figure 4: HaCaT lipid were extracted and analyzed using HPLC/HR-MS and HPLC/Corona. The evolution of lipid biomarkers during keratinocytes differentiation was studied. Ratios of chromatographic peak area of glucosylceramides/ceramides and of sphingomyelins /ceramides calculated at different cells collection step.

View Article Online
DOI: 10.1039/D1AN00231G

Discussion and conclusion

In this study, we induced keratinocytes cell differentiation and followed the process over two weeks using HaCaT cells grown *in vitro* as a 2D cell culture model. Both Raman microspectroscopy and HPLC/HR-MS enabled the detection of several modifications in cell morphology. We also observed spectral signal and biomolecular changes during differentiation and underlined some lipid biomarkers (glucosylceramides and sphingomyelins). Morphological, spectral and biomolecular changes contributed altogether to determine of the differentiation stage. Results demonstrated the ability of HaCaT cells to differentiate *in vitro* (2D) till observing stratified layers, but we did not observe the formation of fully stratified layers, the latter can be obtained when using a 3D culture model.

Our data demonstrated clear biomolecular changes between D9 and D13, which may indicate the passage from the SG to the SC layer. In fact, literature indicates that after 3 weeks of incubation in a low-calcium concentration medium (0.03 mM), HaCaT cells proliferate, take a spindle shape but fail to stratify and to develop intracellular contact. This observation confirm the ability of HaCaT cells to revert back to a basal-like state – under a low-calcium concentration – as previously reported[12, 18]. In contrast, to induce the differentiation process, HaCaT cells should be subjected to a high-concentration of calcium (2.8 mM). Two hours later, they start to take a more cuboidal shape with cell-cell contact[15]. These modifications occur to achieve the morphological characteristics of suprabasal layers[15, 18] . In addition, the stratification layers and the flatter shape of several cells, which were observed at D9 and D13, may indicate the achievement of suprabasal layers but do not enable to determine morphologically the exact stage of keratinocyte differentiation. Wilson *et al.,* reported that the morphological modification should be confirmed biochemically by immunoblotting and immunofluorescence of protein and genes which are known as differentiation markers such as keratin-1 and involucrin[8].

View Article Online
DOI: 10.1039/D1AN00231G

In this work, we are interested in demonstrating the morphological changes by following biomolecular modifications involving lipid, protein, and DNA using Raman microspectroscopy. Raman is a very suitable free label technique to follow cell differentiation at single cell level. The comparison of the mean Raman spectra of each differentiation day demonstrated several modifications in the cells' spectra as shown in figure 2 and table 1. A high increase of the 960 cm^{-1} peak was detected after 13 days and particularly at the stratified layers. This peak has previously been assigned to the C-N vibration of saturated ceramides (such as ceramide III)[22]. In fact, in the outermost epidermal layer, ceramides are the dominant lipid class by weight (over 50%) of total lipids species besides free fatty acids (FFA) and cholesterol [9]. High ceramide content is considered as a marker of the SC layer. Ceramide class consists of fatty acid chains linked to a sphingoid base. Since in the human SC, the FFA are predominantly saturated[41-43], this may explain the high increase in saturated ceramides at the late stage of differentiation. This observation was also confirmed as shown in table (1), by the 3059 cm^{-1} peak at corresponding to the =C-H stretching, this peak decreased during differentiation and may indicate a decrease in the unsaturation chain, related to unsaturated ceramides. In addition, the high increase of the Raman peak at (960 cm^{-1}) is also related to an increase in the ν (C–C) β-sheet keratin conformation[23]. The SC layers (corneocytes) are rich in keratin filament, and a strong increase of the keratin component is a marker of SC layers[23] .

When the keratinocytes reach the SC layer, they lose their nucleus and acquire a flatter shape to become corneocytes[7, 44, 45]. Raman spectral images of HaCaT during differentiation permitted to follow the DNA/lipid ratio (773-790 cm^{-1}/ 2820-2890 cm^{-1}) as shown in figure 3. Our results confirm the decrease of this ratio during the differentiation until it reaches its lowest value at D13. This observation is also confirmed by the characteristic band of nucleic acids at 725 cm^{-1} which decreased significantly at the last day (table 1). The decrease in the nucleic acids levels may confirm the achievement of a later stage of differentiation (SC).

Lipids are mainly found in the cell membrane zone. During keratinocytes differentiation, lipid biosynthesis evolves at early stages and forms at advanced stages the inter-corneocytes matrix of the *stratum corneum*.

View Article Online
DOI: 10.1039/D1AN00231G

In this study, the evolution of the lipid/protein (2820-2890) / (2900-2970) cm^{-1} ratio is an important marker to determine the keratinocytes differentiation stage. As shown in figure 3, after 3 days of high-calcium exposure, this ratio recorded a high increase throughout the cell (except the nucleus zone) indicating a high lipid content compared to that of the proteins. In contrast, the decrease in the intensity at D6 and D9 could be due to an increase in the protein content such as keratin at this stage of differentiation. As shown in table (1), the Raman peak at 1658 cm^{-1}, which is related to the amide I of protein (α helix of keratin), significantly increased at D9. The highest and most homogeneous lipid / protein ratio was observed at D13 (figure 3). This increase reveals the formation of the inter-corneocytes lipid matrix (at the SC) which consists in particular of ceramides, cholesterol and free fatty acids. Literature links this increase to the decrease in the protein content subjected to the proteases of the SC – such as caspase 14 which contributes to the metabolization of filaggrin (involved in the terminal differentiation of keratinocytes and the formation of the cornified envelope in the *stratum corneum*) – leading to less (intact) protein in the outermost layers of the SC[25, 46].

We also followed the evolution of lipid biomarkers during differentiation as shown in figure 4 by HPLC/corona & HPLC/HR-MS. Sphingomyelins and glucosylceramides are recognized as markers of the SG layer[11]. An increase in the glucosylceramides/ceramides and sphingomyelins/ceramides ratio was observed during differentiation. These ratios reached their maximum value at D9, and then started to decrease. This observation indicates the passage of keratinocytes from the SG (high glucosylceramides and sphingomyelins content at D9) to the SC layer (D 13).

To conclude, HaCaT cells subjected to a high-calcium concentration medium differentiated *in vitro* but did not show fully stratified layers. We detected, according to our 2D cell culture model, several modifications occurring at single cell level during differentiation. Our results demonstrate that Raman microspectroscopy is an efficient methodology that allows a free staining observation of epidermal cells. It is a powerful

View Article Online
DOI: 10.1039/D1AN00231G

technique to follow the biomolecular changes including lipid, protein, and DNA evolution with a high ability to determine their location throughout the cells. The complementary information obtained from both Raman microspectroscopy and (HPLC/corona & HPLC/HR-MS) clearly demonstrated molecular modifications between D9 and D13. Indeed, HaCaT cells presented a high increase in lipid and keratin contents, a decrease in DNA and proteins, and a decrease in the ratio of glucosylceramides/ceramides and sphingomyelins/ceramides between D9 and D13. All these observations characterize the differentiation of HaCaT cells and their passage from SG to SC between these two days. In perspective, conducting further data processing by combing Raman and chromatographic data might be interesting[47].

Acknowledgements

The authors would like to thank the SILAB - Jean PAUFIQUE Corporate Foundation of the financial support for this work. We also thank Dr Franck Bonnier for his valuable help.

Compliance with ethical standards Conflict of interest

The authors declare that they have no conflict of interest.

View Article Online
DOI: 10.1039/D1AN00231G

References

1. B. Breiden, H. Gallala, T. Doering and K. Sandhoff, *Eur J Cell Biol*, 2007, **86**, 657-673.
2. D. D. Bikle, Z. Xie and C. L. Tu, *Expert Rev Endocrinol Metab*, 2012, **7**, 461-472.
3. L. Eckhart, S. Lippens, E. Tschachler and W. Declercq, *Biochim Biophys Acta*, 2013, **1833**, 3471-3480.
4. A. Seo, N. Kitagawa, T. Matsuura, H. Sato and T. Inai, *Histochem Cell Biol*, 2016, **146**, 585-597.
5. M. Kypriotou, M. Huber and D. Hohl, *Exp Dermatol*, 2012, **21**, 643-649.
6. J. A. Bouwstra, P. L. Honeywell-Nguyen, G. S. Gooris and M. Ponec, *Prog Lipid Res*, 2003, **42**, 1-36.
7. M. Weil, M. C. Raff and V. M. Braga, *Curr Biol*, 1999, **9**, 361-364.
8. V. G. Wilson, *Methods Mol Biol*, 2013, **1195**, 33-41.
9. Y. Mizutani, S. Mitsutake, K. Tsuji, A. Kihara and Y. Igarashi, *Biochimie*, 2009, **91**, 784-790.
10. A. Kihara, *The Journal of Biochemistry*, 2012, **152**, 387-395.
11. M. Rabionet, K. Gorgas and R. Sandhoff, *Biochimica Et Biophysica Acta-Molecular and Cell Biology of Lipids*, 2014, **1841**, 422-434.
12. A. F. Deyrieux and V. G. Wilson, *Cytotechnology*, 2007, **54**, 77-83.
13. L. Micallef, 'UNIVERSITE DE LIMOGES 2009.
14. P. J. Houghton, P. J. Hylands, A. Y. Mensah, A. Hensel and A. M. Deters, *J Ethnopharmacol*, 2005, **100**, 100-107.
15. D. D. Bikle, *J Cell Biochem*, 2004, **92**, 436-444.
16. S. E. Lee and S. H. Lee, *Ann Dermatol*, 2018, **30**, 265-275.
17. L. Verzeaux, R. Vyumvuhore, D. Boudier, M. Le Guillou, S. Bordes, M. Essendoubi, M. Manfait and B. Closs, *Exp Dermatol*, 2017, DOI: 10.1111/exd.13388.
18. S. Pillai, D. D. Bikle, M. L. Mancianti, P. Cline and M. Hincenbergs, *J Cell Physiol*, 1990, **143**, 294-302.
19. E. G. Bligh and W. J. Dyer, *Can J Biochem Physiol*, 1959, **37**, 911-917.
20. A. Mieremet, M. Rietveld, S. Absalah, J. van Smeden, J. A. Bouwstra and A. El Ghalbzouri, *PLoS One*, 2017, **12**, e0174478.
21. A. Assi, J. Bakar, D. Libong, E. Sarkees, A. Solgadi, A. Baillet-Guffroy, R. Michael-Jubeli and A. Tfayli, *Anal Bioanal Chem*, 2019, DOI: 10.1007/s00216-019-02301-3.
22. A. Tfayli, E. Guillard, M. Manfait and A. Baillet-Guffroy, *Anal Bioanal Chem*, 2010, **397**, 1281-1296.
23. C. Choe, J. Schleusener, J. Lademann and M. E. Darvin, *Sci Rep*, 2017, **7**, 15900.
24. M. Gniadecka, O. Faurskov Nielsen, D. H. Christensen and H. C. Wulf, *J Invest Dermatol*, 1998, **110**, 393-398.
25. M. Janssens, J. van Smeden, G. J. Puppels, A. P. Lavrijsen, P. J. Caspers and J. A. Bouwstra, *Br J Dermatol*, 2014, **170**, 1248-1255.
26. L. Verzeaux, R. Vyumvuhore, D. Boudier, M. Le Guillou, S. Bordes, M. Essendoubi, M. Manfait and B. Closs, *Exp Dermatol*, 2017, **27**, 403-408.
27. S. Tfaili, C. Gobinet, G. Josse, J. F. Angiboust, M. Manfait and O. Piot, *Analyst*, 2012, **137**, 3673-3682.
28. G. Zhang, D. J. Moore, C. R. Flach and R. Mendelsohn, *Anal Bioanal Chem*, 2007, **387**, 1591-1599.
29. N. Garcia, O. Doucet, M. Bayer, D. Fouchard, L. Zastrow and J. P. Marty, *Int J Cosmet Sci*, 2002, **24**, 25-34.
30. Z. Movasaghi, S. Rehman and I. U. Rehman, *Applied Spectroscopy Reviews*, 2007, **42**, 493-541.

View Article Online
DOI: 10.1039/D1AN00231G

31. N. Stone, C. Kendall, J. Smith, P. Crow and H. Barr, *Faraday Discuss*, 2004, **126**, 141-157; discussion 169-183.
32. A. D. Meade, O. Howe, V. Unterreiner, G. D. Sockalingum, H. J. Byrne and F. M. Lyng, *Faraday Discuss*, 2016, **187**, 213-234.
33. L. Franzen and M. Windbergs, *Adv Drug Deliv Rev*, 2015, **89**, 91-104.
34. S. Tfaili, C. Gobinet, G. Josse, J. F. Angiboust, A. Baillet, M. Manfait and O. Piot, *Anal Bioanal Chem*, 2013, **405**, 1325-1332.
35. H. Wang, T. H. Tsai, J. Zhao, A. M. Lee, B. K. Lo, M. Yu, H. Lui, D. I. McLean and H. Zeng, *Photodermatol Photoimmunol Photomed*, 2012, **28**, 147-152.
36. S. Tfaili, A. Al Assaad, N. Fournier, F. Allaoui, J. L. Paul, P. Chaminade and A. Tfayli, *Talanta*, 2019, **199**, 54-64.
37. R. Vyumvuhore, A. Tfayli, H. Duplan, A. Delalleau, M. Manfait and A. Baillet-Guffroy, *Analyst*, 2013, **138**, 4103-4111.
38. C. Choe, J. Schleusener, J. Lademann and M. E. Darvin, *J Biophotonics*, 2018, **11**, e201700355.
39. K. Czamara, K. Majzner, M. Z. Pacia, K. Kochan, A. Kaczor and M. Baranska, *Journal of Raman Spectroscopy*, 2015, **46**, 4-20.
40. M. Egawa, K. Tokunaga, J. Hosoi, S. Iwanaga and Y. Ozeki, *Journal of biomedical optics*, 2016, **21**, 86017.
41. M. N. Ansari, N. Nicolaides and H. C. Fu, *Lipids*, 1970, **5**, 838-845.
42. L. Norlen, I. Nicander, A. Lundsjo, T. Cronholm and B. Forslind, *Arch Dermatol Res*, 1998, **290**, 508-516.
43. J. van Smeden and J. A. Bouwstra, *Curr Probl Dermatol*, 2016, **49**, 8-26.
44. O. Lopez, M. Cocera, P. W. Wertz, C. Lopez-Iglesias and A. de la Maza, *Biochim Biophys Acta*, 2007, **1768**, 521-529.
45. D. T. Downing, *J Lipid Res*, 1992, **33**, 301-313.
46. C. Capallere, C. Plaza, C. Meyrignac, M. Arcioni, M. Brulas, V. Busuttil, I. Garcia, E. Bauza and J. M. Botto, *Toxicol In Vitro*, 2018, **53**, 45-56.
47. R. Vyumvuhore, A. Tfayli, O. Piot, M. Le Guillou, N. Guichard, M. Manfait and A. Baillet-Guffroy, *J Biomed Opt*, 2014, **19**, 111603.